Scenarios for LHC/FCC Based Gamma-Proton Colliders

Zafer Nergiz[a,*], Saleh Sultansoy[b,c], Husnu Aksakal[d], Frank Zimmermann[e]

[a] *Nigde Omer Halisdemir University, Faculty of Arts and Sciences, Department of Physics, 51200 Nigde, Turkey*
[b] *TOBB University, Ankara, Turkey*
[c] *Institute of Physics, Academy of Sciences, Baku, Azerbaijan*
[d] *Kahramanmaras Sutcu Imam University, Kahramanmaras, Turkey*
[e] *CERN, Switzerland*

Abstract

The advantage of the linac-ring type electron proton collider is that it allows for the straightforward construction of γp collider. In a γp collider high energy photons can be generated from Compton backscattering of laser photons off electrons from a linear accelerator. In this study main parameters of photon-proton colliders based on some future electron linear accelerator projects and protons supplied form LHC or FCC are evaluated.

Keywords: LHC, FCC, LHeC, CLIC, ILC, PWFA-LC, photon-proton colliders.

---

1. Introduction

Linac-Ring type ep colliders seems to be sole realistic way to handle Multi-TeV center of mass energy in electron proton collisions [1]. Today 60 GeV energy recovery linac is considered as baseline option both for LHC and FCC based ep colliders [2]. On the other hand energy frontier options using one pass linacs have a huge potential for BSM physics search [3].

Combination of several future linear accelerator projects with LHC (Large Hadron Collider) and FCC (Future Circular Collider) offers a unique opportunity to build γp colliders [3, 4, 5]. γp collisions allow investigations of extremely low x and high Q^2 physics in quantum chromodynamics. Physics search potential of γp colliders at a new kinematic range is reviewed in references [6, 7, 8, 9].

In the photon colliders ($\gamma\gamma$, γe, γp and γA), high energy photons are produced by the Compton backscattering of the intense laser pulse off the electron beam provided by the linear accelerator [10, 11, 12]. In our case, the backscattered photons are generated at conversion point (CP) and are collided with protons at interaction point (IP). A schematic view of a γp collider is shown in Fig. 1.

2. Compton Backscattering

Compton cross section is characterized by a dimensionless parameter given by [13]

$$x = \frac{4E_b\omega_0}{m_e^2} Cos^2\left(\frac{\alpha_0}{2}\right) , \tag{1}$$

where E_b is the initial energy of electrons, ω_0 is the energy of a laser photon and α_0 is the collision angle between laser beam and electron beam. In the case of head on collision and with practical units, Eq. (1) can be written as $x = 15.3E_b[TeV]\omega_0[eV]$. The energy of backscattered photons increases with increasing value of the parameter x. However, if x is larger than 4.8, high energy photons can be lost due to e^+e^-

---

[*] Corresponding Author tel: +903882254080
Email address: `znergiz@ohu.edu.tr` (Zafer Nergiz)

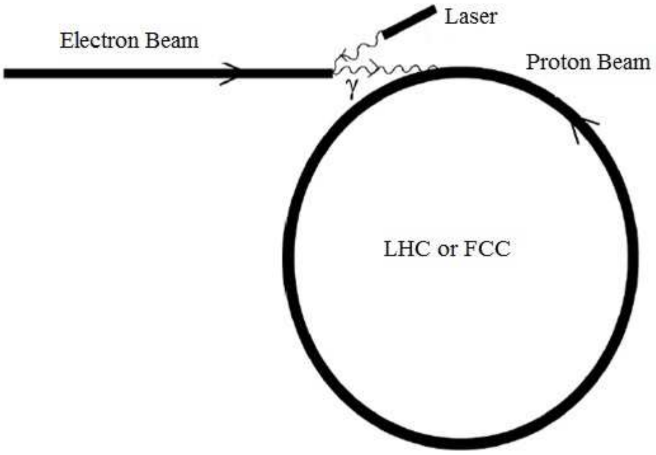

Figure 1: Schematic view of γp colliders.

pair creation in collisions of backscattered photons with unscattered laser photons. Maximum energy of backscattered photons is $\omega_{max} = E_b x/(x+1)$. For x=4.8 and neglecting nonlinear Compton scattering process, maximum photon energy is $0.83\times E_b$.

As the laser photon density increases, the collision probability of two or more laser photons with a high energy electron is increases as well. Therefore, in the strong electromagnetic fields at the laser focus, nonlinear Compton scattering process given by

$$e^- + n\gamma_{laser} \to e^- + \gamma\ , \quad (n \geq 1) \tag{2}$$

becomes important. This nonlinear effect is characterized by the parameter

$$\xi^2 = n_\gamma \left(\frac{4\pi\alpha}{m_e^2\omega_0}\right), \tag{3}$$

where n_γ is the laser photon density, α is fine structure constant and m_e is electron mass. Considering nonlinear Compton scattering process, maximum energy of backscattered photons produced by electron colliding with n laser photons is given by [14]

$$\omega_{max}^n = E_b \frac{nx}{1+\xi^2+nx}. \tag{4}$$

Another process, which affects the backscattered photon spectrum is successive scattering. To obtain the effects of the successive scattering, simulation program is needed.

3. Luminosity of LHC/FCC Based γp Colliders

Two hadron colliders (LHC and FCC) with several lepton collider projects (ILC, CLIC and PWFA-LC) as well as ERL 60 offer the possibility to realize γp colliders in different range of energy. The energy spectra of backscattered photons from different linear accelerator projects and luminosity spectra of different linac×LHC/FCC based γp colliders are investigated by using CAIN simulation code [15].

3.1. Linear collider projects

Because of the high energy losses of electrons due to the synchrotron radiation, two linear accelerator projects for future lepton colliders have priority: ILC (International Linear Collider) and CLIC (Compact Linear Collider).

The ILC is designed as a 500 GeV center-of-mass energy linear electron-positron collider based on superconducting radio-frequency technology and can be extended to 1 TeV [16].

CLIC is a future collider project to provide e^+e^- collisions with normal conducting high frequency (12 G Hz) rf structure. The CLIC is planned to construct in three stage: 0.380 TeV, 1.5 TeV and 3 TeV center of mass energy, respectively [2]. Besides this three stages, 60 GeV option was also proposed in ref. [17]. Recently, using multiple delay loops and rf deflectors have been proposed to match the bunch structure of proton beam and CLIC 60 GeV [18]. The electron beam will has 312 bunches with 25 ns spacing and 25 beam pulses spaced 6 μs repeating at 100 Hz. Therefore, the collision frequency of $312 \times 25 \times 100$ can be achieved. In this paper upgraded version of 60 GeV option is choosen for CLIC as electron source.

LHeC (Large Hadron electron Collider) is a project which aim to interact the 60 GeV electrons with LHC's protons. As electron source, Energy Recovery Linac (ERL) is proposed to provide high electron average current and increase the luminosity [19]. The ERL can also be used for e source for compton backscattering process. However, because of the energy losses of 65% of electrons after conversion region the Energy Recovery Process should be bypassed. In that case the average electron beam current of the electron linac can be 0.3 mA.

Recently, more compact linear collider based beam driven plasma wake field technology is proposed. In PWFA-LC proposal, extremely high electron beam energy of 5 TeV can be realized with relatively low cost and high efficiency [20].

The mentioned linac parameters are shown in Tables 2 and 3.

3.2. Laser requirements

If the multiple scattering is neglected and assuming that the laser profile seen by each electron is the same, the conversion probability of generating high energy gamma photons per individual electron can be written as [21]

$$p = 1 - e^{-q}, \tag{5}$$

where

$$q = \frac{\sigma_c A}{\omega_0 \Sigma_L}, \tag{6}$$

where A is laser pulse energy, ω_0 is laser photon energy, Σ_L is the transverse area of laser spot and σ_c is the Compton cross section which is $1.75 \times 10^{-25} cm^2$ for x=4.8. Proposed laser parameters are given in Table 1

Table 1: Laser parameters for the 60 GeV ERL Options and CLIC, 500 GeV ILC and 5000 GeV PWFA-LC.

Parameters	ERL and CLIC	ILC	PWFA-LC
Laser wavelength (μm)	0.24	2.0	20
Pulse Energy (J)	10	2	8
Pulse length (mm)	1	0.3366	2.5
Rayleigh length (mm)	0.5	0.5	3.5
ξ^2	0.05	0.23	0.16

Backscattered photon spectra obtained from CAIN simulation code are shown in Figs. 2, 3, 4 and 5. A peak seen at low energies is a result of the successive scattering. The spreads at high energy regions in the spectra are due to the nonlinear Compton backscattering effect.

3.3. LHC based γp colliders

While the proton-proton collisions is running at LHC (Large Hadron Collider), the design studies on several post-LHC hadron collider projects are studied at CERN: HE-LHC (High Energy LHC), HL-LHC (High Luminosity LHC) and FCC (Future Circular Collider) options [2]. The High-Luminosity LHC is an approved luminosity upgrade of the LHC. The High Energy LHC aimed to reach the beam energy around 13.5 TeV in the existing LHC tunnel by using 16.0 Tesla FCC dipole magnets instead of LHC's 8.33 Tesla

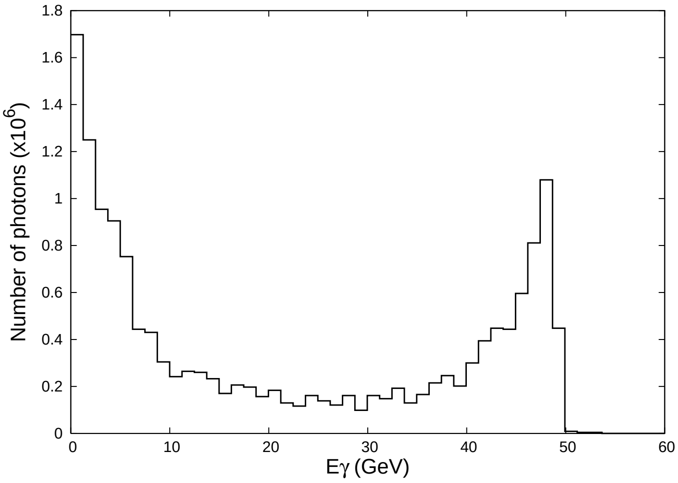

Figure 2: Backscattered photon spectrum from LHeC-ERL Linac.

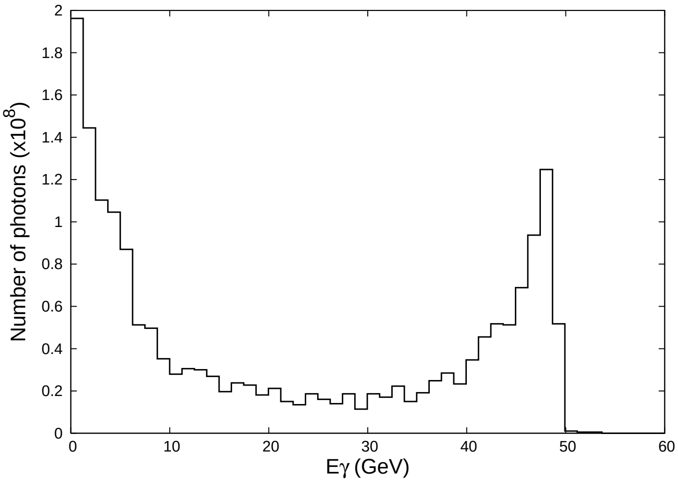

Figure 3: Backscattered photon spectrum from CLIC 60 GeV Linac.

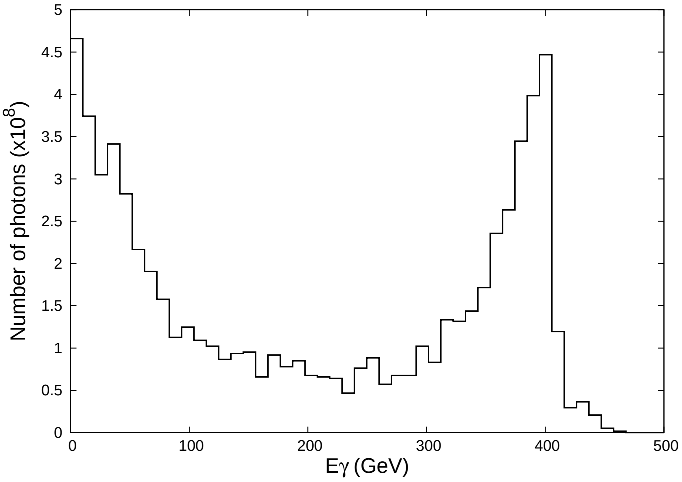

Figure 4: Backscattered photon spectrum from ILC Linac.

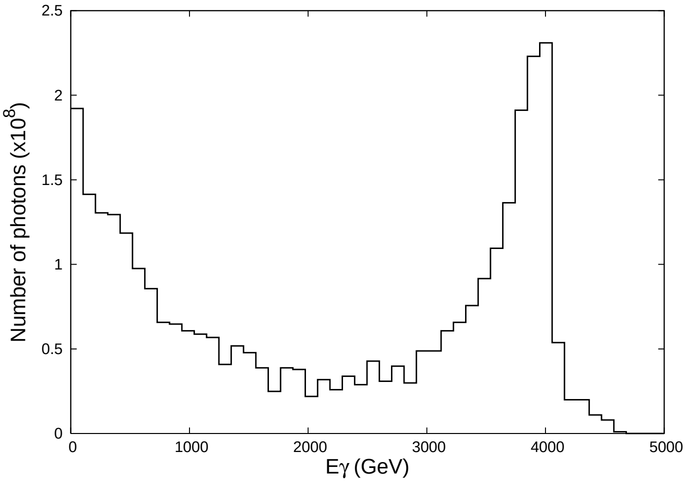

Figure 5: Backscattered photon spectrum from PWFA-LC Linac.

nominal dipol magnets. The proposed linacs and LHC options beam parameters are given in Table 2. The parameters for LHeC CDR, HL-LHC and HE-LHC parameters updated from ref. [2] according to the γp colliders requirements.

Table 2: Proposed accelerator parameters for different e-LHC based γp colliders.

Parameters	LHeC CDR	ep at HL-LHC	ep at HE-LHC	CLIC-LHC	ILC-LHC	PWFA-LHC
E_p (TeV)	7	7	12.5	7	7	7
E_e (GeV)	60	60	60	60	500	5000
Max. C.M.E (TeV)	1.17	1.17	1.6	1.17	3.40	10.75
Bunch spacing (ns)	25	25	25	25	366 (350)	2×10^5
Protons per bunch (10^{11})	1.7	2.2	2.5	2.5	2.2	2.2
ε_p (μm rad)	3.7	2	2.5	3.7	3.7	3.7
IP β_p^* (cm)	10	7	10	10	10	10
Pr. bunch length (mm)	75.5	75.5	75.5	75.5	75.5	75.5
Electrons per bunch (10^9)	0.045	0.045	0.045	5.2	17.4	10.0
Electron current (mA)	0.3	0.3	0.3	0.64	0.027	0.008
ε_e (μm rad)	5	5	5	5	10	50
IP β_e^* (cm)	120	44	44	120	470	960
El. bunch length (mm)	0.21	0.21	0.21	0.21	0.225	0.020
Collision Frequency (s^{-1})	40×10^6	40×10^6	40×10^6	78×10^4	9800	5000
CP to IP distance (cm)	100	100	100	100	100	100
Tot. Luminosity ($10^{30}cm^{-2}s^{-1}$)	6.2	10.0	11.7	14.0	2.5	0.6
Lum. 0.9-1 W_{max}($10^{30}cm^{-2}s^{-1}$)	4.4	8.3	9.8	10.0	0.8	0.2

The luminosity distribution in terms of $W_{\gamma p}$ center of mass energy is

$$\frac{dL_{\gamma p}}{dW_{\gamma p}} = \frac{W_{\gamma p}}{2E_p}\frac{N_\gamma N_p f_{coll}}{2\pi(\sigma_e^2+\sigma_p^2)} f(\frac{W_{\gamma p}^2}{4E_p}) exp[-\frac{z^2\theta_\gamma(\frac{W_{\gamma p}^2}{4E_p})^2}{2(\sigma_e^2+\sigma_p^2)}] \tag{7}$$

where Ep is proton beam energy, $f(\frac{W_{\gamma p}^2}{4E_p})$ signifies the differential Compton cross section, $N\gamma$ is the number of back scattered photons per pulse, Np is the protons per bunch, f_{col} is collision frequency, σ_e anf σ_p are transverse beam sizes electrons and protons, $\theta_\gamma(\frac{W_{\gamma p}^2}{4E_p})$ are angle of backscattered photons and z is the distance between conversion and interaction points [4]. The luminosity spectrum of gamma proton collider is strongly related with the distance between the conversion and interaction points. As it can be seen in Fig. 6 by increasing the distance the total luminosity is decreasing. However, the spectrum become more monochromatic. At high energies the effect of the distance on the luminosity is relatively low. Another advantage of the long distance is to make relatively easier extraction of the spent electrons. Therefore the CP to IP distance is chosen 100 cm for all LHC based collider options. Luminosity spectra of γp colliders based on LHeC and LHC options are shown inFig. 7. The luminosity spectra for ILC×LHC and PWFA-LC×LHC are presented in Figs. 8 and 9, respectively.

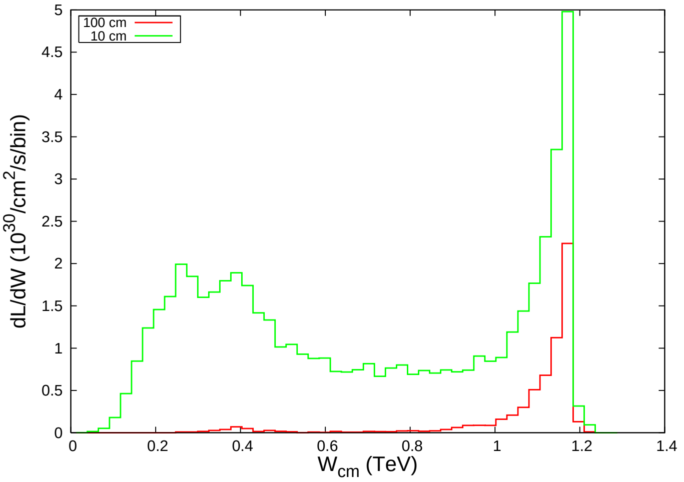

Figure 6: Comparison of Luminosity spectra of LHeC ERL×LHC for short and long CP to IP distance.

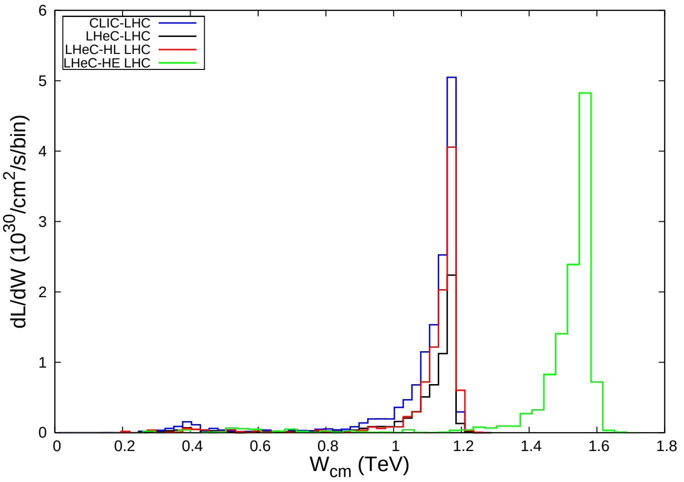

Figure 7: Luminosity spectra for LHeC ERL×LHC, LHeC ERL×HL-LHC, LHeC ERL×HE-LHC and CLIC×LHC.

3.4. FCC based γp colliders

FCC is the future project, which includes pp collider with 100 TeV center-of-mass energy, supported by European Union within the Horizon 2020 Framework Program for Research and Innovation [22]. Proposed linacs and FCC beam parameters for γp colliders based on FCC are given in Table 3. The bunch spacing of ILC is greater than FCC's bunch spacing. Therefore, most of the proton bunches would not interact with ILC's electrons. However, number of protons per bunch can be increased by decreasing the number of

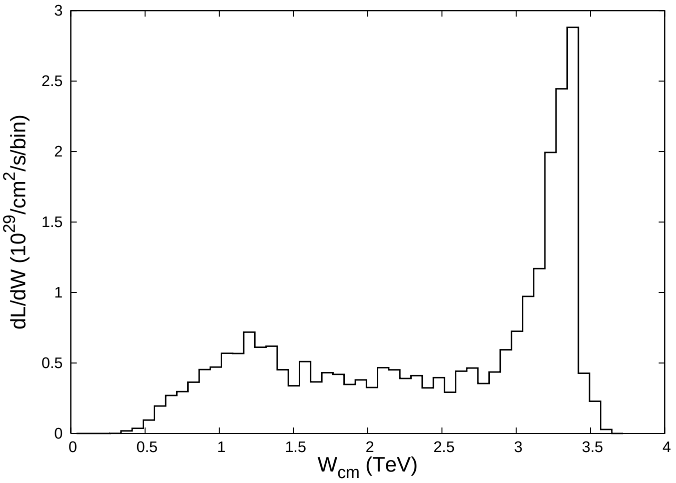

Figure 8: Luminosity spectrum for ILC×LHC.

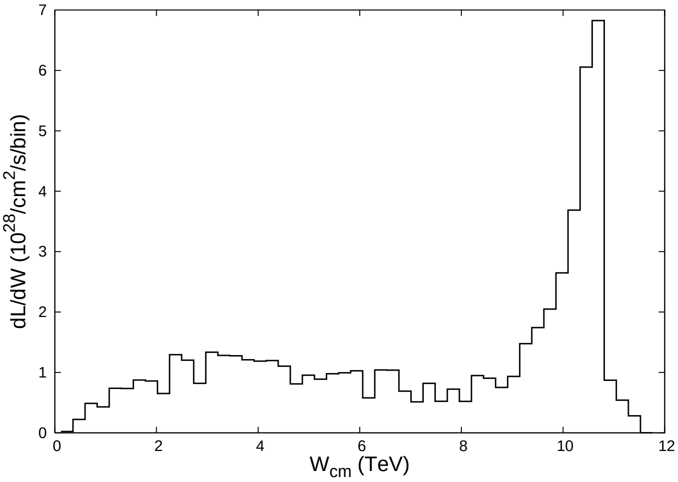

Figure 9: Luminosity spectrum for PWFA-LC×LHC.

proton bunches. Upgraded parameters are shown in the table in parenthesis. Same upgrade also applied for PWFA-LC×FCC. Luminosity spectra of proposed LHC based γp colliders are shown in Figs. 10, 11, 12 and 13.

Table 3: Proposed accelerator parameters for different e-FCC based γp colliders.

Parameters	FCC-eh	CLIC-FCC	ILC-FCC	PWFA-FCC
E_p (TeV)	50	50	50	50
E_e (GeV)	60	60	500	5000
Max. C.M.E (TeV)	3.14	3.14	9	28.7
Bunch spacing (ns)	25	25	366 (350)	2×10^5
Protons per bunch (10^{11})	1.0	1	1.0 (2.2)	1.0 (2.2)
ε_p (μm rad)	2.2	2.2	2.2	2.2
IP β_p^* (cm)	15	15	10	10
Pr. bunch length (mm)	75.5	75.5	75.5	75.5
Electrons per bunch (10^9)	0.045	5.2	17.4	10
Electron current (mA)	0.3	0.64	0.027	0.008
ε_e (μm rad)	5	5	10	50
IP β_e^* (cm)	14	14	40	80
El. bunch length (mm)	0.210	0.21	0.225	0.020
Collision Frequency (s^{-1})	40×10^6	78×10^4	9800	5000
CP to IP distance (cm)	30	30	100	100
Tot. Luminosity ($10^{30}cm^{-2}s^{-1}$)	91.0	200	16	5.2
Lumi. 0.9-1W_{max}($10^{30}cm^{-2}s^{-1}$)	50	114	8.3	1.9

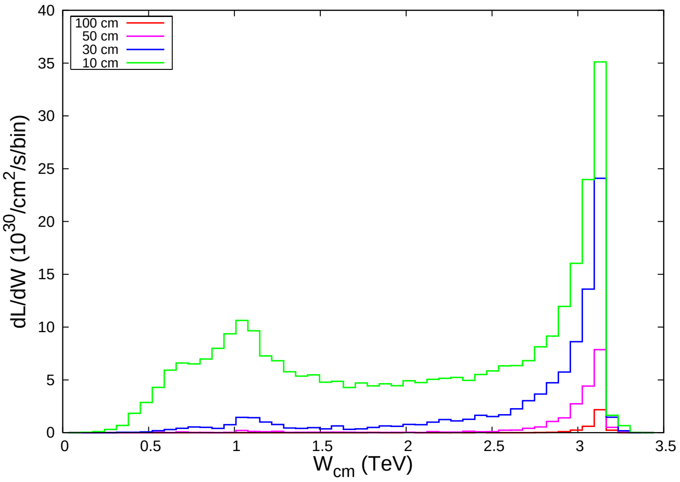

Figure 10: Luminosity spectrum for LHeC ERL×FCC for different CP to IP distances.

4. Physics at γp colliders

Analyses performed for UNK+VLEPP [23], HERA+LC [24], THERA [25] and LHeC [19] have shown superiority of γp colliders compared with corresponding ep colliders for a lot of SM and BSM phenomena (small x gluon, anomalous interactions of t quark, q* and so on). Similar studies should be performed for FCC based γp colliders. Below we list several examples of physics phenomena where γp colliders have a huge potential.

Concerning BSM physics, polarization of high energy photon beam (for details see [4, 7]) will give an opportunity to determine Lorentz structure of γqq^*, γqt ,γWW and γZZ vertices. It is important that

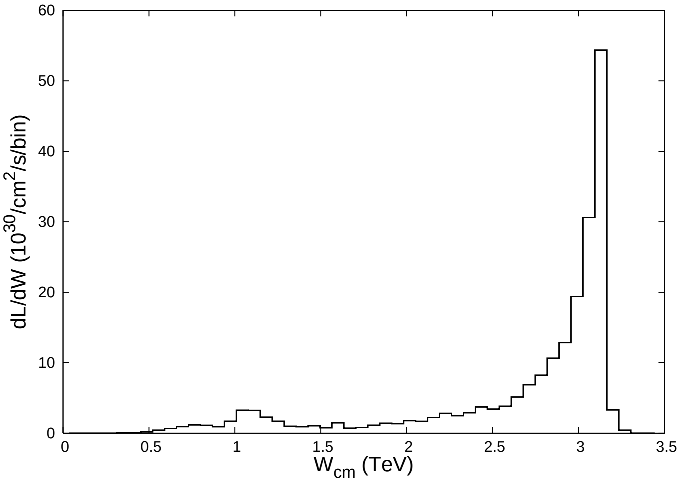

Figure 11: Luminosity spectrum for CLIC×FCC.

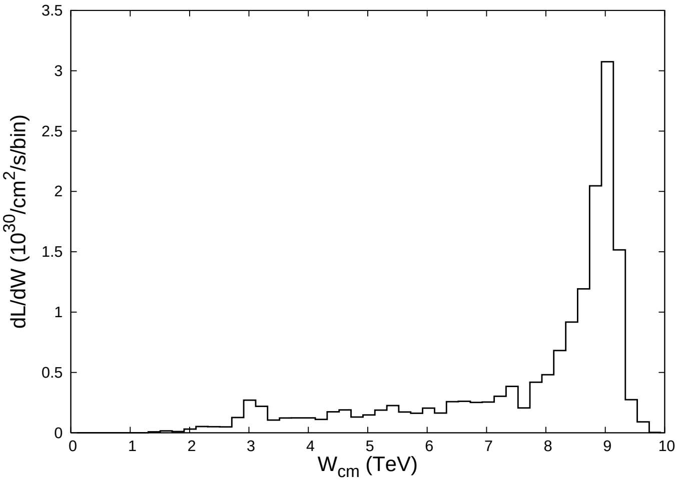

Figure 12: Luminosity spectrum for ILC×FCC.

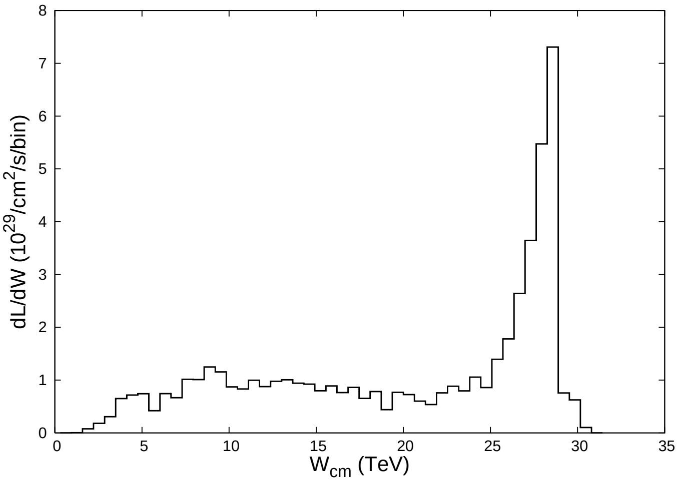

Figure 13: Luminosity spectrum for PWFA-LC×FCC.

at γp colliders we deal with pure photon interactions, whereas at ep colliders both γ and Z contribute to corresponding processes and their interactions cannot be separated.

As for SM physics, γp colliders will give opportunity to measure total cross-sections of interaction of real photons with matter at very high energies comparable with cosmic γ-rays. Then, investigation of the process $\gamma p \to bbX$ will give opportunity to clarify QCD basics: $Q^2 \geq 4m_b^2 \approx 100\,GeV^2$ means perturbative QCD while $x_g \approx 4(m_b^2)/\sqrt{s_{\gamma p}}$ (see Table 4) correspond to high density of gluons (saturation region).

Table 4: Characteristic x_g values for pair production of c and b quarks at different γp colliders.

Protons	LHC			FCC		
Electrons	ERL	ILC	PWFA	ERL	ILC	PWFA
$\bar{c}c$	10^{-5}	10^{-6}	10^{-7}	10^{-6}	10^{-7}	10^{-8}
$\bar{b}b$	10^{-4}	10^{-5}	10^{-6}	10^{-5}	10^{-6}	10^{-7}

5. Conclusion

Lepton-hadron collider with $\sqrt{s_{ep}}$ of order of 1 TeV (multi-TeV) is necessary both to clarify fundamental aspects of the QCD part of the Standard Model and for adequate interpretation of experimental data from the LHC (FCC-hh). Furthermore, linac-ring type ep colliders will provide an opportunity to construct γp colliders with $\sqrt{s_{\gamma p}} \approx 0.9\sqrt{s_{ep}}$.

In this paper, we have described the design parameters, including laser requirements, for p colliders based on LHC and FCC. The effect of distance between conversion and interaction points has been analyzed: more distance means more monochromaticity but less luminosity.

Certainly, multi-TeV scale γp collider have a huge search potential for both SM and BSM physics and essentially enlarge capacity of basic ep collider. In order to clarify this potential, systematic study of different physics phenomena is needed. We cordially invite HEP community to start this study.

6. Acknowledgment

This work was supported by the Turkish Atomic Energy Agency with Grant No. 2015 TAEK (CERN) A5.H6.F2-13 and also, in part, by the European Commission under the HORIZON2020 Integrating Activity project ARIES, grant agreement 730871.

References

[1] A. N. Akay, H. Karadeniz, S. Sultansoy., Review of linac-ring-type collider proposals, International Journal of Modern Physics A 25 (2010) 4589–4602. `doi:{10.1142/S0217751X10049165}`.

[2] F. Bordry, M. Benedikt, O. Bruning, J. Jowett, L. Rossi, D. Schulte, S. Stapness, F. Zimmermann, Machine parameters and projected luminosity performance of proposed future colliders at CERN, Tech. rep., CERN-ACC-2018-0037, Geneva, Switzerland (2018).

[3] Y. C. Acar, A. N. Akay, S. Beser, A. C. Canbay, H. Karadeniz, U. Kaya, B. B. Oner, S. Sultansoy, Future circular collider based leptonhadron and photonhadron colliders: Luminosity and physics, Nucl. Instr. Meth. Phys. Res. A 871 (2017) 47–53. `doi:{10.1016/j.nima.2017.07.041}`.

[4] H. Aksakal, A. K. Ciftci, Z. Nergiz, D. Schulte, F. Zimmermann, Conversion efficiency and luminosity for gamma-proton colliders based on the LHC-CLIC or LHC-ILC QCD explorer scheme, Nucl. Instr. Meth. Phys. Res. A 576 (2007) 287–293. `doi:{10.1016/j.nima.2007.03.019}`.

[5] H. Aksakal, A. K. Ciftci and Z. Nergiz, High energy photon beam generation for QCD explorer based gamma p colliders , in: AIP Conf.Proc. 899, 2007, 183-184.

[6] S. Sultansoy, Four ways to TeV scale, Turk J. Physics 22 (1998) 575–594.

[7] A. K. Ciftci, S. Sultansoy, S. Turkoz, O. Yavas, Main parameters of TeV energy gp colliders, Nucl. Instr. Meth. Phys. Res. A 365 (1995) 317–328. `doi:{10.1016/0168-9002(95)00674-5}`.

[8] E. Arik, S. Sultansoy, Turkish comments on 'Future perspectives in HEP' , hep-ph/0302012.

[9] S. Sultansoy, Linac-ring type colliders: Second way to TeV Scale, Eur. Phys. J. C 33 (2004) 1064–1066.

[10] V. I. Telnov, Problems in obtaining gg and ge colliding beams at linear colliders , Nucl. Instr. Meth. Phys. Res. A 294 (1990) 72– 92. `doi:{10.1016/0168-9002(90)91826-W}`.

[11] V. I. Telnov, Principles of photon colliders , Nucl. Instr. Meth. Phys. Res. A 335 (1995) 3– 18. `doi:{10.1016/0168-9002(94)01173-7}`.

[12] D. L. Borden, D. A. Bauer, D. O. Caldwell, Physics possibilities at a photon linear collider, SLAC-PUB 5715 (1992) 1–52.

[13] I. F. Ginzburg, G. L. Kotkin, V. G. Serbo, V. I. Telnov, Colliding ge and gg beams based on the single pass e^+e^- colliders (VLEPP Type) , Nucl. Instr. Meth. 205 (1983) 47– 68. `doi:{10.1016/0167-5087(83)90173-4}`.

[14] M. Galynskii, E. Kuraev, M. Levchuk, V. I. Telnov, Principles of photon colliders , Nucl. Instr. Meth. Phys. Res. A 472 (2001) 267–279. `doi:{10.1016/S0168-9002(01)01195-0}`.

[15] K. Yokoya, Users Manual of CAIN, Tech. rep., https://ilc.kek.jp/ yokoya/CAIN/Cain242/CainMan242.pdf (2011).

[16] C. Adolphsen, et al., The International Linear Collider technical design report, Tech. rep., arXiv:1306.6328 (2013).

[17] D. Schulte, F. Zimmermann, QCD Explorer based on LHC and CLIC-1, Tech. rep., CERN-AB-2004-079 (2004).

[18] D. Schulte, F. Zimmermann, Potential performence of LHeC based on CLIC, 2018, Electron for the LHC workshop, LAL Orsay.

[19] J. L. A. Fernandez, et al., A Large Hadron Electron Collider at CERN, Journal of Phyics G- Nuclear and Particle Physics 39 (2012) 075001. `doi:{10.1088/0954-3899/39/7/075001}`.

[20] J. P. Delahaye, E. Adli, S. Gessner, M. Hogan, T. Raubenheimer, W. An, C. Joshi, W. Mori, A beam driven plasma-wakefield linear collider from higgs factory to multi-tev, in: Proceedings of the Fifth International Particle Accelerator Conference, 2014, Dresden, Germany, p. 3791.

[21] C. Adolphsen, et al., Zeroth-Order Design Report for the Next Linear Collider, Tech. rep., LBNL5424, SLAC474 (1996).

[22] M. Benedikt, D. Schulte, F. Zimmermann, Optimizing integrated luminosity of future hadron colliders, Phys. Rev. Spec. Top. Accel. Beams 18 (2015) 101002. `doi:{10.1103/PhysRevSTAB.18.101002}`.

[23] S.I. Alekhin, E.E. Boos, V.I. Borodulin, G.V. Jikia, S.R. Slabospitsky, A. Yu. Smirnov, S.F. Sultanov, Physics at γp colliders of TeV energies, Int. J. Mod. Phys. A 6 (1991) 21–40. `doi:{10.1142/S0217751X91000034}`.

[24] Z. Z. Aydin, A. K. Ciftci, S. Sultansoy, HERA + LC based gamma p collider: Luminosity and physics, Int. J. Mod. Phys. A 11 (1996) 2019–2044. `doi:{10.1142/S0217751X96001024}`.

[25] Edited by U. Katz, M. Klein, A. Levy, S. Schlenstedt, The THERA Book, Tech. rep., DESY-LC-REV-2001-062 (2001).